Journal of Alloys and Compounds 561 (2013) 161–173

Contents lists available at SciVerse ScienceDirect

Journal of Alloys and Compounds

journal homepage: www.elsevier.com/locate/jalcom

Experimental study of the Cu–Ni–Y system at 700 °C using diffusion couples and key alloys

Mohammad Mezbahul-Islam *, Mamoun Medraj

Department of Mechanical Engineering, Concordia University, 1455 de Maisonneuve Blvd. West, Montreal, Quebec, Montreal, Canada H3G 1M8

ARTICLE INFO

Article history:
Received 6 November 2012
Received in revised form 31 January 2013
Accepted 1 February 2013
Available online 16 February 2013

Keywords:
Ternary isothermal section
Diffusion couple
X-ray diffraction
Wave dispersive X-ray spectrometer
Hydrogen storage
Metallic glass

ABSTRACT

Two solid–solid diffusion couples and 29 key samples have been used to construct the isothermal section of the Cu–Ni–Y system at 700 °C. Phase relations and ternary solubility of the binary compounds have been determined using scanning electron microscopy (SEM), wave dispersive X-ray spectrometer (WDS) and X-ray diffraction (XRD) analysis. The isothermal section at 700 °C consists of two single-phase region, 21 two-phase regions and 10 three-phase regions. Two extended solid solutions, between CuY*–NiY and Cu_4Y–Ni_4Y have been determined. The maximum solubility of Ni in Cu_2Y, Cu_7Y_2 and Cu_6Y has been found to be about 28, 7.5 and 3.9 at.% Ni, respectively. The solubility of Cu in NiY_3, Ni_2Y, Ni_3Y, Ni_7Y_2, Ni_5Y and $Ni_{17}Y_2$ is about 12.04, 9.67, 25, 3.08, 75 and 37 at.%. Cu, respectively. The solubility of Y in fcc (Cu, Ni) phase is about 0.6 at.%.

1. Introduction

Rare earth (RE)–Ni based alloys are promising candidates for the hydrogen storage and magnetic materials [1,2]. $Ni_{2.5}Cu_{0.5}Y$ has been found to be a good hydrogen storage material [1]. $Ni_{17}Y_2$ has shown some magnetic characteristics with the addition of small amount of Cu [2]. Also, the Cu–Ni–Y is a constituent ternary of the Mg–Cu–Ni–Y which is an important metallic glass forming system [3,4]. A combination of experimental measurements and computational methods is an efficient approach to determine the phase equilibria in multi-component systems. A self-consistent thermodynamic database provides essential information for developing new alloys. For instance, the impact of adding certain amount of Cu or Mg to $Ni_{2.5}Cu_{0.5}Y$ or any other composition with respect to temperature or pressure can be easily calculated. However, experimental knowledge of the actual phase equilibria is required for the construction of such database. Therefore, the main aim of this work is to provide a clear idea about the phase relations in the Cu–Ni–Y system for the whole composition range.

Only limited amount of work has been done on this system. Zheng and Nong [6] reported a partial isothermal section ($Y \leqslant 16.7$ at.%) at room temperature based on their XRD results of key alloys. They reported two three phase equilibrium regions among Cu_6Y, Ni_5Y and fcc (Cu,Ni) phases and Ni_5Y, $Ni_{17}Y_2$ and fcc (Cu,Ni) phases. Although, Cu_5Y does not exist in the accepted Cu–Y binary phase diagram, they proposed complete solubility between Ni_5Y and Cu_5Y. They also reported the solubility of $Ni_{17}Y_2$ to be about 35 at.% Cu and the maximum solubility of Y in the fcc (Cu, Ni) phase to be less than 1.5 at.% Y. Kadomatsu et al. [7] studied the structural phase transitions in $Cu_{1-x}Ni_xY$ alloys using electrical resistivity measurements at normal and high pressures, thermal expansion and X-ray analysis. They reported that the CsCl type CuY phase changes to FeB type structure at low temperature. This phase transition takes place with a very large thermal hysteresis. While heating, it was found that the low temperature phase (FeB type) is stable up to 510 °C while during cooling, it was stable down to −153 °C. Burnasheva and Tarasov [1] studied the hydrogen storage capacity of Ni_3Y by partially replacing Ni with other transition elements. They found Ni_3Y to be stable untill 16.67 at.% Cu at 497 °C. Paul-Boncour et al. [8] studied the $(Ni,Cu)_2Y$ pseudobinary compounds for the structural change of the cubic Ni_2Y phase to the orthorhombic Cu_2Y phase using XRD, neutron diffraction, density measurement and electron microprobe analysis. They reported that about 20% of Ni can be substituted by Cu while preserving the cubic superstructure of $Ni_2Y_{0.95}$ while 50% of Cu can be replaced by Ni in the orthorhombic Cu_2Y structure at 750 °C. Dwight [9] studied the crystal structures of several $Cu_xNi_{5-x}Y$ alloys to understand the solubility of the Ni_5Y compound by XRD. According to their report Ni_5Y has a solubility of about 66.67 at.% Cu at 800 °C. All these results will be compared with the present investigation. A summary of the previous work on this system up to 1994 has been done by Gupta [10]. The crystal struc-

* Corresponding author. Tel.: +1 514 848 2424x3146; fax: +1 514 848 3175.
E-mail address: mmedraj@encs.concordia.ca (M. Mezbahul-Islam).

0925-8388/$ - see front matter © 2013 Elsevier B.V. All rights reserved.
http://dx.doi.org/10.1016/j.jallcom.2013.02.011

ture of the binary phases of the Cu–Ni–Y system has been documented in the Pearson database [5] as listed in Table 1.

In the literature, a few binary compounds in this system were reported to dissolve the third element. This needs to be confirmed. The solubility of all other binary compounds will be investigated here. Gupta [10] proposed a complete mutual solubility between CuY* and NiY. This also needs to be confirmed. Finally, the equilibrium phase relations need to be understood. In-order to clarify all these issues it is decided to experimentally investigate the Cu–Ni–Y system and construct the 700 °C isothermal section for the whole composition range. Also it is worth emphasizing that in the current work a combination of many experimental techniques have been used to obtain as accurate results as possible; whereas in the literature one experimental technique was used at a time to study this system.

2. Experimental procedure

In order to establish the phase relations and identify the ternary solubility two solid–solid diffusion couples were utilized. The diffusion couple is a powerful and efficient technique for mapping the phase diagram of ternary systems [11–13]. It also eliminates the problems associated to alloy preparation especially systems with high melting temperatures [14]. Within the diffusion layers the equilibrium phases occur, whereas at the interface local equilibrium takes place [14]. However, one should always consider the possibility of missing phases [14,15] while using diffusion couple for determining phase diagram. This may occur because of the slow nucleation of the phase which prevents formation of the diffusion layer. In order to obtain more reliable information, Kodentsov et al. [14] suggested to combine the diffusion couple method with key sample analysis. Therefore, in the present work both of these techniques have been used.

The key alloys were prepared in an arc melting furnace using water cooled copper crucible under flowing argon. The purity of the elements used is Cu – 99.99%, Ni – 99.99%, and Y – 99.9%, all supplied by Alfa Aesar. The furnace chamber was evacuated and purged by argon several times before melting. Each alloy was crushed and remelted at least four times to ensure homogeneity. The actual global composition of the samples was identified by Inductively Coupled Plasma–Optical Emission Spectrometry (ICP–OES). The solid–solid diffusion couple was prepared from two end member blocks of ternary alloys. Contacting surfaces of these blocks were pre-grinded down to 1200 grit using SiC paper and polished with 1 μm diamond paste and 99% ethanol as a lubricant. The blocks were pressed together using clamping rings, placed in a Ta container and sealed in a quartz tube under protective Ar atmosphere. The key alloys and diffusion couples were annealed at 700 °C for 6 weeks. Although higher annealing temperature is desirable for faster kinetics, it should be chosen below the lowest melting temperature of the alloy system to avoid melting during annealing. In the present work, the annealing temperature has been chosen based on the lowest eutectic of the three pertinent binary systems. Among the three binaries the lowest eutectic occurs in the Cu–Y system at around 800 °C. Therefore, it is decided to anneal the samples at 700 °C to reach equilibrium faster without melting. These alloys were then characterized by light optical microscopy, scanning electron microscopy (SEM) and wave dispersive X-ray spectrometer (WDS) using point and line scans. The error of the WDS measurements was estimated to be around ±2 at.%. The XRD patterns were obtained using PANanalytical Xpert Pro powder X-ray diffractometer with a Cu Kα radiation. The XRD spectrum is acquired from 20° to 120° 2θ with a 0.02° step size. XRD analysis of the samples is carried out using X'Pert HighScore Plus Rietveld analysis software.

3. Results and discussion

3.1. Diffusion couples

Backscatter electron (BSE) images of the solid–solid diffusion couple-1 annealed at 700 °C for 6 weeks with gradually increased magnification of the area of interest are shown in Fig. 1a–c. The end member 1 (Cu/Ni/Y 80.90/14.13/4.97 at.%) is a two phase region of fcc and Ni_5Y. The other end member (Cu/Ni/Y 15.90/9.10/75.0 at.%) consists of a three phase region of CuY*, NiY_3 and hcp-Y. These two end members are closer to the Cu–Y side, one with high Cu concentration and the other with high Y concentration. They were chosen in order to identify the ternary solubility of the binary compounds of the Cu–Y system.

During heat treatment, extensive interdiffusion of Cu, Ni and Y took place allowing various equilibrium phases to form. A WDS line scan was used to determine the solubility ranges of Cu_2Y and CuY*, as shown in Fig. 1a. Spot analysis was carried out to deduce the composition of the two phase (NiY_3 + CuY*) region. On the basis of the compositional information, the solid solubility of the binary compounds extending into ternary system was evaluated. Benefitting from the local equilibrium at the interfaces formed between diffusion layers, the sequence of phases along the diffusion path was deduced as: {fcc (Cu, Ni) + Ni_5Y}(end member) → Ni_5Y → Ni_5Y + Cu_2Y → Cu_2Y → Cu_2Y + CuY* → CuY* → CuY* + NiY_3 → {CuY* + NiY_3 + hcp-Y} (end member). Fig. 1d shows the estimated diffusion path projected on the Cu–Ni–Y Gibbs triangle.

Fig. 2, summarizes the results of 1.125 mm WDS line scan across two diffusion layers (Cu_2Y and CuY*) and spot analysis of the other zones. The diffusion layer of the Ni_5Y phase kept breaking during polishing and was difficult to analyze by WDS line scan. However, spot WDS analysis was possible on a few Ni_5Y retained regions. The next layer is very stable and is about 1 mm thick. It represents the ternary solubility of Cu_2Y. The line scan of this layer shows almost constant concentration of the three constituents as shown in Fig. 2. It is probably because of the distinctive location

Table 1
Binary phases of the Cu–Ni, Cu–Y and Ni–Y systems and their structure data [5].

Phase	Pearson's symbol	Space group	Type	Lattice parameters (Å)		
				a	b	c
fcc (Cu, Ni)	cF4	$Fm\bar{3}m$	Cu			
αY	hP2	$P6_3/mmc$	Mg			
βY	cI2	$Im\bar{3}m$	W			
Cu_6Y	h	–	–	6.83	–	4.07
Cu_4Y	hp6	$P6_3/mmc$	$CaCu_5$	4.994	–	4.113
Cu_7Y_2	–	–	–	–		
Cu_2Y	oI12	Imma	$CaCu_2$	4.305	6.800	7.315
CuY	cP2	$Pm\bar{3}m$	CsCl	3.477		
CuY*	oP8	Pnma	FeB			
$Ni_{17}Y_2$	hp38	$P6_3/mmc$	Th_2Ni_{17}	8.307		8.040
Ni_5Y	hp6	P6/mmm	$CaCu_5$	4.883		3.967
Ni_4Y	–	–	–	–		
Ni_7Y_2	hR18	$R\bar{3}m$	Gd_2Co_7	4.924		36.67
Ni_3Y	hR12	$R\bar{3}m$	$PuNi_3$	5.000		4.300
Ni_2Y	cF24	$Fd\bar{3}m$	Cu_2Mg	7.181	4.100	5.510
NiY	oP8	Pnma	FeB	7.120	4.100	5.510
Ni_2Y_3	tp80	P4,2,2	Ni_2Y_3	7.104		3.659
NiY_3	oP16	Pnma	Fe_3C	6.920	4.470	6.360

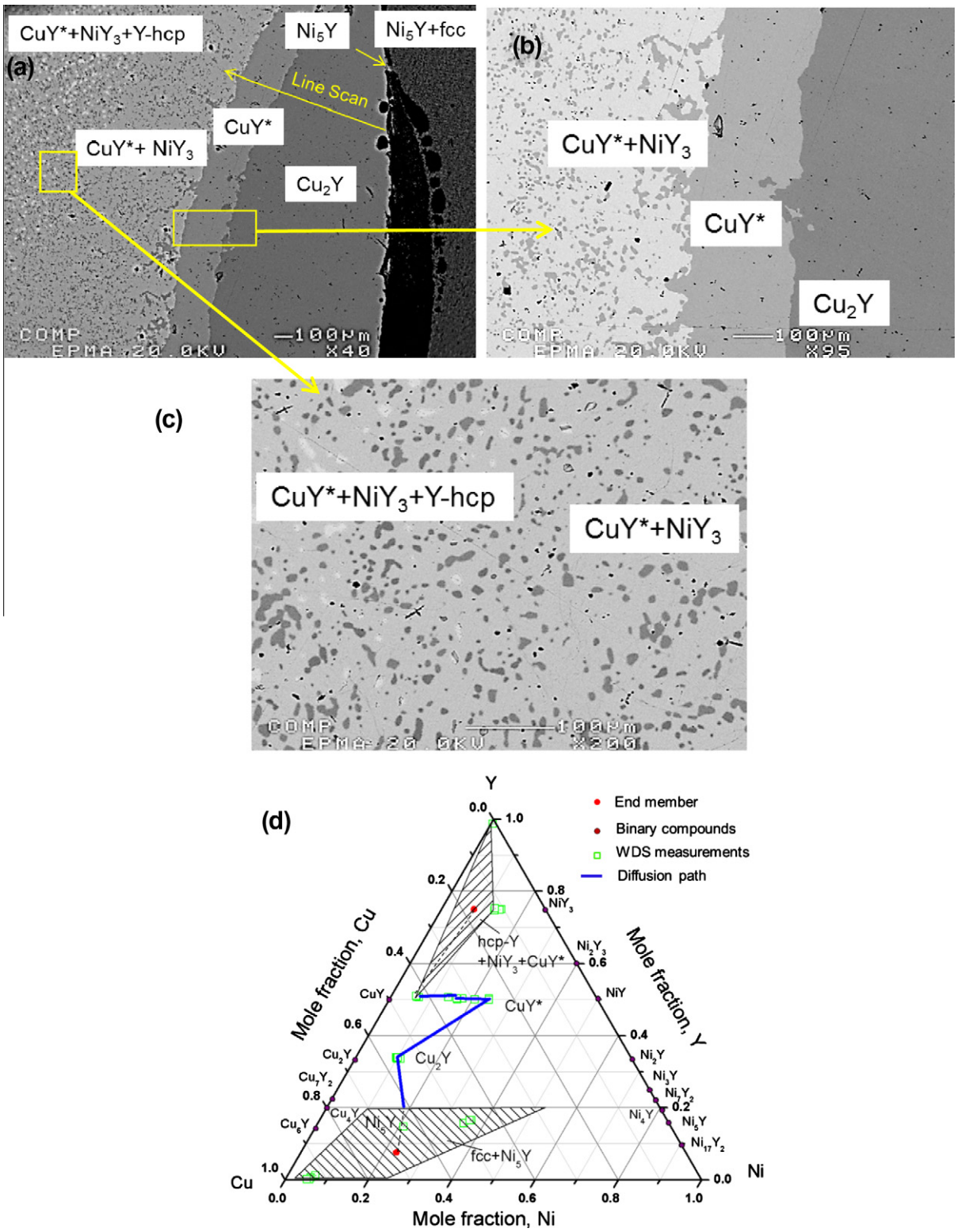

Fig. 1. (a–c) BSE images of the solid–solid diffusion couple-1 annealed at 700 °C for 6 weeks, showing the formation of four intermetallic compounds; and (d) diffusion path projected on the Cu–Ni–Y Gibbs triangle.

of the end members (a line connecting the two end members is almost perpendicular to the solubility line) which does not allow diffusion path to move horizontally. Therefore, it forms a thick layer with almost constant composition. The layer after this is about 100 μm and represents the CuY* phase. The concentration profile of this layer (Fig. 2) reveals that the CuY* phase forms a substitutional solid solution where Cu substitutes for Ni atoms while the Y content remains constant at ~50 at.%. The interface of the two layers (CuY* and Cu_2Y) represents two phase region due to the precipitation of the Cu_2Y phase. The next layer is a two phase region between CuY* and NiY_3 phase. The concentration profile in Fig. 2 for the two phase region of CuY*+NiY_3 has been obtained by spot

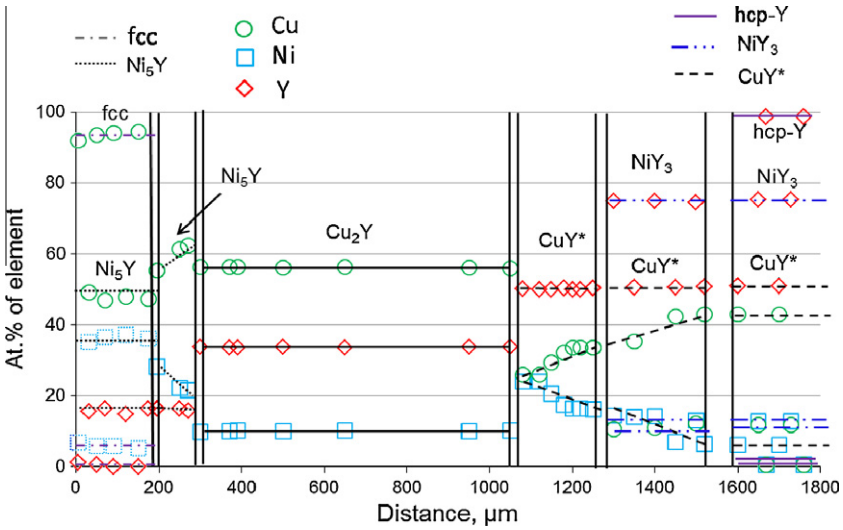

Fig. 2. Composition profile of the diffusion couple 1 along the line scan shown in Fig. 1a. Different phases have been represented by different line type for clear understanding.

analysis of the phases taking measurements at approximately equal distances through a line perpendicular to the interface. The profile shows constant Y concentrations of ~50 and ~75 at.% in CuY^* and NiY_3, respectively. However, variation in the Cu and Ni concentrations can be observed for CuY^*. As can be seen in Fig. 2 in the $NiY_3 + CuY^*$ region, the concentration of Cu is increasing and that of Ni is decreasing. This reveals the substitution of Ni by Cu. After this the three phase region ($CuY^* + NiY_3$ + hcp-Y) of the end member can be seen. The maximum solubility of Cu in NiY_3 has been found to be ~10.5 at.% Cu. However, no solubility of Cu or Ni in the hcp-Y phase could be observed.

No phases can be found between the Ni_5Y and Cu_2Y layer, which is not in agreement with key sample analysis in this region that suggests the presence of Cu_4Y phase. This is probably due to the highly stable Cu_2Y phase which hinders the diffusion of Y atoms to the next layer. However, the diffusion couple approach does not always give successful results when it is used to determine phase diagrams. The possibility of missing phase is a common phenomenon [14]. In order to overcome this uncertainty, a combined investigation with key samples has been followed and will be discussed.

The BSE image of the 2nd solid–solid diffusion couple is shown in Fig. 3a and b. The diffusion path is shown in Fig. 3c. The end member 1 (Cu/Ni/Y 30.47/62.16/7.37 at.%) is a two phase region of fcc and $Ni_{17}Y_2$. The other end member (Cu/Ni/Y 22.67/47.13/30.20 at.%) consists of three phases; Cu_2Y, Ni_2Y and Ni_3Y. The end members are chosen close to each other in this fashion in order to force the formation of the intermetallic layers of Ni_5Y, Ni_4Y and Ni_3Y. Two diffusion layers can be seen clearly in the BSE image. The WDS analysis identifies these two layers as Ni_5Y and Ni_3Y. A line scan has been done through these two layers and the compositional profile is shown in Fig. 4. A careful observation of the profile shows the presence of the Ni_4Y phase in between Ni_5Y and Ni_3Y. The Y content in this layer has been found to be constant at about 20.9 at.% while Ni atoms were substituted by Cu atoms. The solubility of the Cu in Ni_4Y was observed to be from about 30–40 at.% Cu.

The sequence of phases along the diffusion path was deduced as: {fcc + $Ni_{17}Y_2$} (end member) → Ni_5Y → $Ni_5Y + Ni_4Y$ → Ni_4Y → $Ni_4Y + Ni_3Y$ → Ni_3Y → {$Ni_3Y + Ni_2Y + Cu_2Y$} (end member). The first diffusion layer is about 12 μm thick and is identified as Ni_5Y phase. The next layer is very thin about 4 μm representing Ni_4Y. The subsequent layer is about 12 μm thick and is identified as Ni_3Y. Because of the small contrast between these two layers (Ni_4Y and Ni_3Y), it was not possible to visualize them separately in the BSE image. After this layer the diffusion path terminates in the three phase region of the end member, $Ni_3Y + Ni_2Y + Cu_2Y$.

3.2. Isothermal section based on key alloys analysis

29 key alloys have been prepared and investigated in order to construct the isothermal section at 700 °C. Based on the WDS and XRD analysis of these alloys and the two diffusion couples, the isothermal section at 700 °C has been constructed as shown in Fig. 5. The phase regions shown by the dotted lines are tentative. The actual global composition of the key alloys and WDS results are summarized in Table 2.

The Cu–Ni system is completely miscible below the liquidus until the critical (T_c) temperature below which the fcc phase changes from a paramagnetic to a ferromagnetic state. On the other hand both Cu–Y and Ni–Y systems have several intermetallic compounds and many of the compositions such as CuY^*–NiY, Cu_2Y–Ni_2Y, Cu_7Y_2–Ni_7Y_2 and Cu_4Y–Ni_4Y show resemblance in terms of their stoichiometry and crystal structure to some extent. Therefore, they have a tendency to form ternary solubility along these lines. These compounds basically sectioned the Cu–Ni–Y system into several pseudo-binary zones. To obtain a clear understanding of various phase relations in the Cu–Ni–Y system, an elaborate discussion on the WDS and XRD results of the key alloys is given below.

3.2.1. Three phase regions

Y-hcp + NiY_3 + CuY^*

A three phase region has been identified among the hcp-Y, NiY_3 and CuY^* phases. CuY^* is referring to the complete mutual solubility between CuY^* and NiY. This solubility will be named as NiY in this paper. The BSE image and XRD pattern of key sample 1 (Cu/Ni/Y 16.08/8.69/75.23 at.%) in Fig. 6a and b clearly show the phase relationship. Based on the WDS analysis listed in Table 2, the maximum solubility of Cu in NiY_3 is found to be 12.0 at.%. Rietveld refinement of the XRD results reveals the lattice parameters as a = 6.93 Å, b = 9.70 Å and c = 6.39 Å.

NiY + Cu_2Y + Ni_2Y

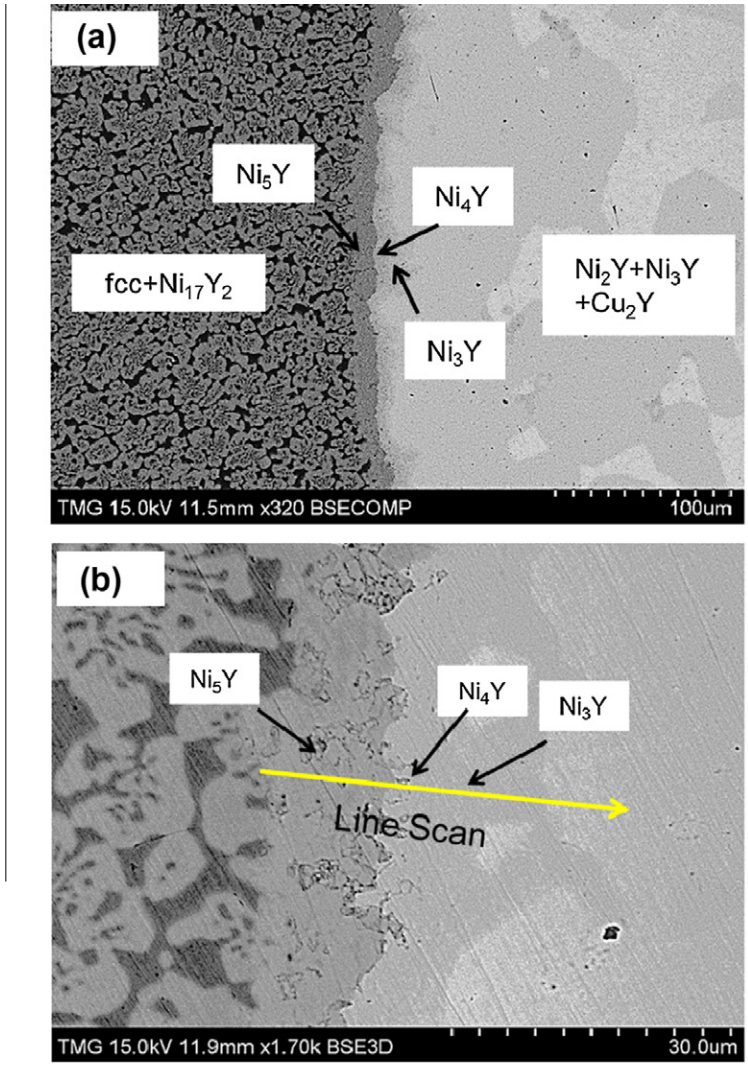

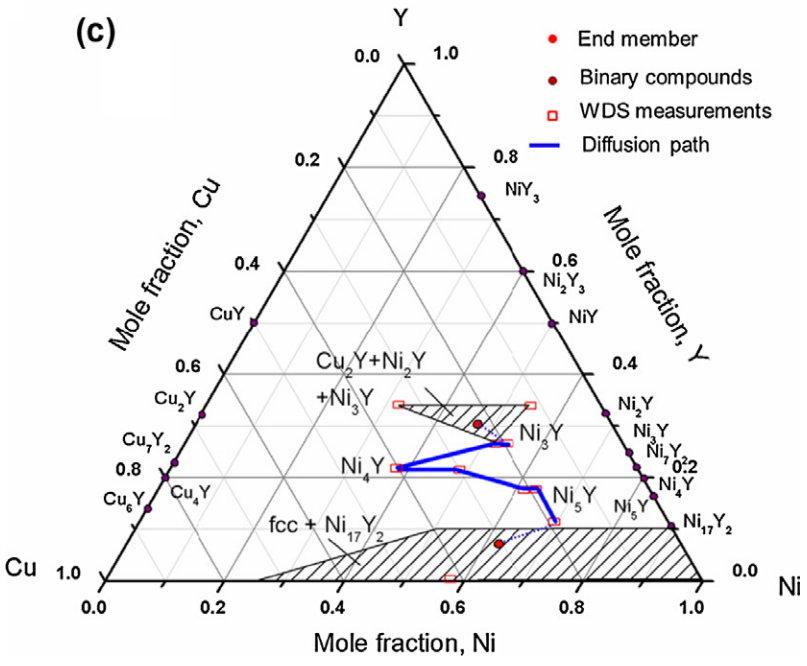

Fig. 3. (a and b) BSE images of the solid–solid diffusion couple 2 annealed at 700 °C for 6 weeks, showing the formation of six intermetallic compounds; and (c) diffusion path in the Cu–Ni–Y Gibbs triangle.

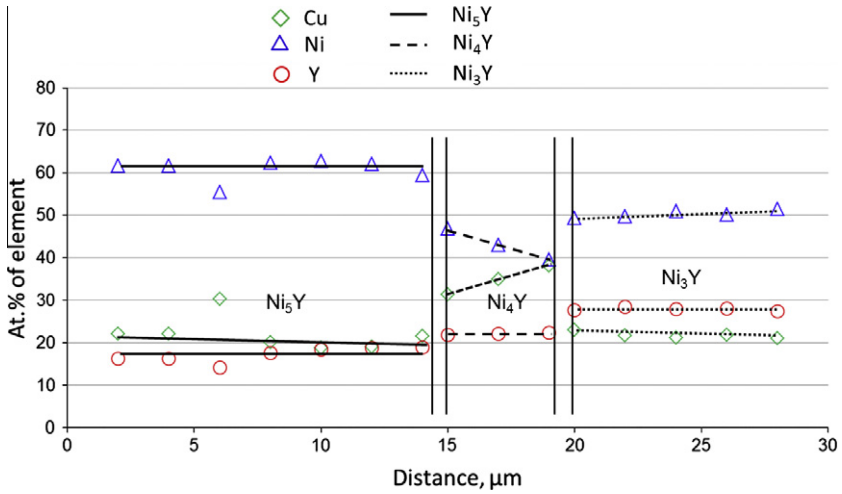

Fig. 4. Composition profile of the diffusion couple 2 along the line scan shown in Fig. 3b. Different phases have been represented by different line types for clear understanding.

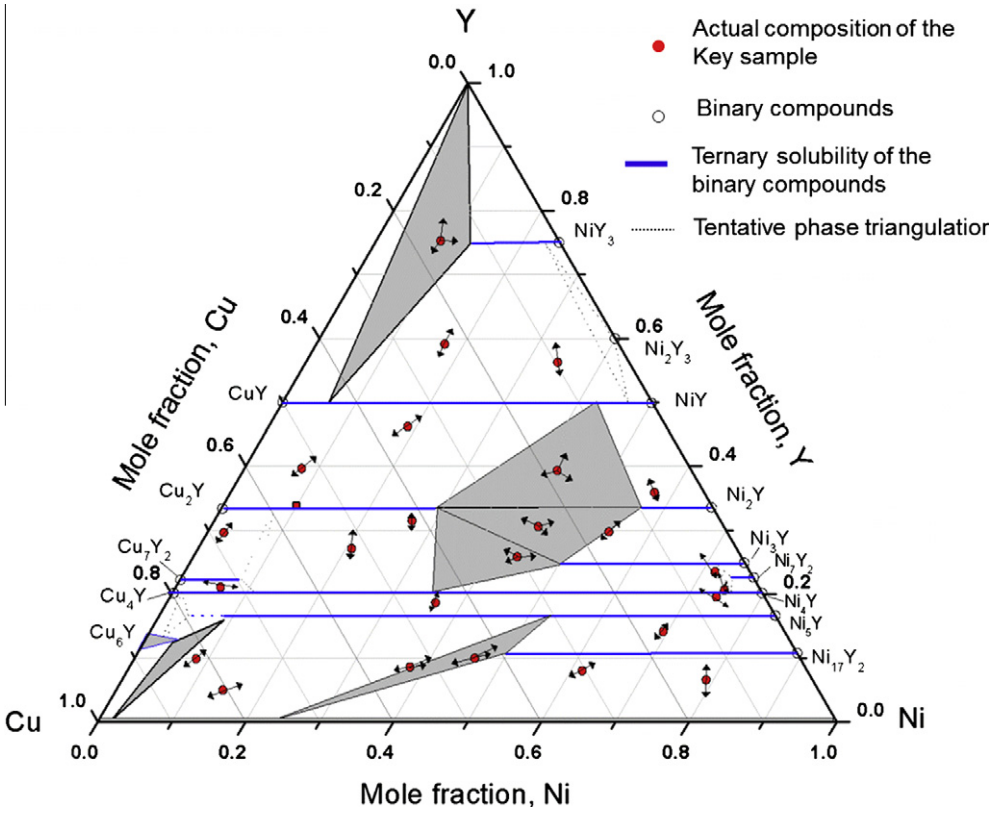

Fig. 5. Isothermal section of the Cu–Ni–Y system at 700 °C. The arrow heads point to the location of the phase composition.

Another three phase region was found among NiY, Cu_2Y and Ni_2Y phases. The BSE image and XRD pattern of sample 6 is shown in Fig. 7a and b. The WDS analysis of this sample is shown in Table 2. The maximum solubility of Cu_2Y and Ni_2Y are found to be 28 at.% Ni and 57 at.% Ni, respectively. These values are in good agreement with those of Paul-Boncour et al. [8] who reported them as 30.5 at.% and 56.25 at.% Ni, respectively.

Observing the variation in the lattice parameters of Cu_2Y is attempted in this work. Rietveld analysis has been performed for the XRD patterns of the five key alloys (4, 5, 6, 9 and 10) that contain Cu_2Y. The change of lattice parameter and cell volume with Ni concentration has been shown in Fig. 8a–d compared with the values reported by Paul-Boncour et al. [8] which shows good agreement. The '*a*' parameter decreases significantly with the increase of Ni concentration due to the smaller atomic size of Ni. The Cell volume also decreases linearly with the increase in Ni concentration. However, negligible change of the '*b*' and '*c*' parameters can be observed. Paul-Boncour et al. [8] analyzed the crystal structure of the Cu_2Y closely using neutron diffraction and XRD experiments. They reported large anisotropic shifting of the atoms due to the substitution. This explains larger increment of the '*a*' parameter than '*b*' and '*c*'.

Table 2
SEM–WDS data on selected Cu–Ni–Y alloys annealed at 700 °C.

Actual composition				Identified phases			
No	(at.%)			Name	Compositions by WDS		
	Cu	Ni	Y		Cu	Ni	Y
1				NiY	43.12	6.19	50.69
	16.08	8.69	75.23	NiY_3	12.04	12.87	75.09
				hcp–Y	0.94	0.53	98.53
2	23.26	17.23	59.51	NiY_3	8.78	16.99	74.23
				NiY	32.34	17.33	50.33
3	8.38	35.51	56.12	NiY_3	2.13	22.28	75.59
				NiY	10.99	36.57	52.44
4	34.92	18.71	46.37	NiY	26.69	22.33	50.98
				Cu_2Y	54.89	9.61	35.5
5	50.81	8.75	40.44	Cu_2Y	60.49	4.13	35.38
				NiY	35.91	12.74	51.34
6	18.15	41.98	39.88	NiY	7.4	42.24	50.36
				Ni_2Y	10.77	57.43	31.8
				Cu_2Y	38.45	28.03	33.52
7	6.68	57.35	35.97	NiY	4.68	44.93	50.39
				Ni_2Y	7.12	60.66	32.21
8	68.17	2.17	29.66	Cu_2Y	61.88	3.21	34.91
				Cu_7Y_2	76.56	1.04	22.41
9	52.13	20.75	27.12	Cu_2Y	47.53	17.68	34.79
				Cu_4Y	55.79	23.01	21.20
10	41.57	26.80	31.62	Cu_2Y	40.79	25.61	33.6
				Cu_4Y	46.65	32.03	21.32
11	30.34	43.78	25.88	Cu_2Y	38.22	27.35	34.43
				Ni_3Y	25.62	48.44	25.94
				Cu_4Y	43.50	35.50	21.00
12	25.10	44.23	30.67	Cu_2Y	33.42	30.96	35.62
				Ni_2Y	12.19	55.57	32.24
				Ni_3Y	20.27	53.34	26.38
13	15.92	54.38	29.70	Ni_2Y	11.33	54.97	33.69
				Ni_3Y	20.36	52.67	26.97
14	72.74	6.03	21.23	Cu_7Y_2	74.52	3.60	21.88
				Cu_4Y	70.27	8.32	21.41
15	77.99	3.48	18.53	Cu_4Y	76.78	3.44	19.78
16	4.68	71.81	23.51	Ni_3Y	6.17	67.04	26.79
				$Ni_{17}Y_2$	5.88	70.55	23.57
17	4.93	74.37	20.70	Ni_4Y	3.06	77.57	19.36
				Ni_7Y_2	4.09	74.09	21.82
				Ni_3Y	4.45	70.76	24.78
18	6.48	73.92	19.60	Ni_4Y	8.44	70.69	20.87
				Ni_5Y	5.64	75.74	18.62
19	85.64	1.37	12.99	Cu_6Y	84.50	1.53	13.97
20	81.78	8.46	9.74	Ni_5Y	72.94	11.66	15.40
				fcc	97.88	1.83	0.30
21	72.38	13.14	14.48	Ni_5Y	70.31	13.70	15.99
				fcc	97.39	0.02	2.59
22	65.57	22.34	12.09	Ni_5Y	52.65	30.65	16.70
				fcc	95.68	4.14	0.18
23	80.90	14.13	4.97	fcc	93.54	5.84	0.62
				Ni_5Y	48.22	35.61	16.17
24	44.96	36.30	18.74	Ni_5Y	46.07	36.38	17.56
				Cu_4Y	43.90	36.05	20.04
25				Ni_5Y	31.98	51.41	16.61
	53.44	37.91	8.65	$Ni_{17}Y_2$	40.27	48.48	11.25
				fcc	83.03	16.88	0.09
26	43.94	45.99	10.07	Ni_5Y	30.61	52.72	16.67
				$Ni_{17}Y_2$	38.00	49.39	12.61
				fcc	76.50	23.06	0.44
27	30.34	61.57	8.08	fcc	45.74	53.64	0.62
				Ni_5Y	23.83	64.65	11.51

(*continued on next page*)

Table 2 (*continued*)

Actual composition				Identified phases			
No	(at.%)			Name	Compositions by WDS		
	Cu	Ni	Y		Cu	Ni	Y
28	13.99	79.60	6.41	$Ni_{17}Y_2$	13.21	76.34	10.45
				fcc	17.9	81.45	0.65
29	16.71	69.17	14.12	Ni_5Y	14.59	69.51	15.90
				$Ni_{17}Y_2$	19.21	68.44	12.35

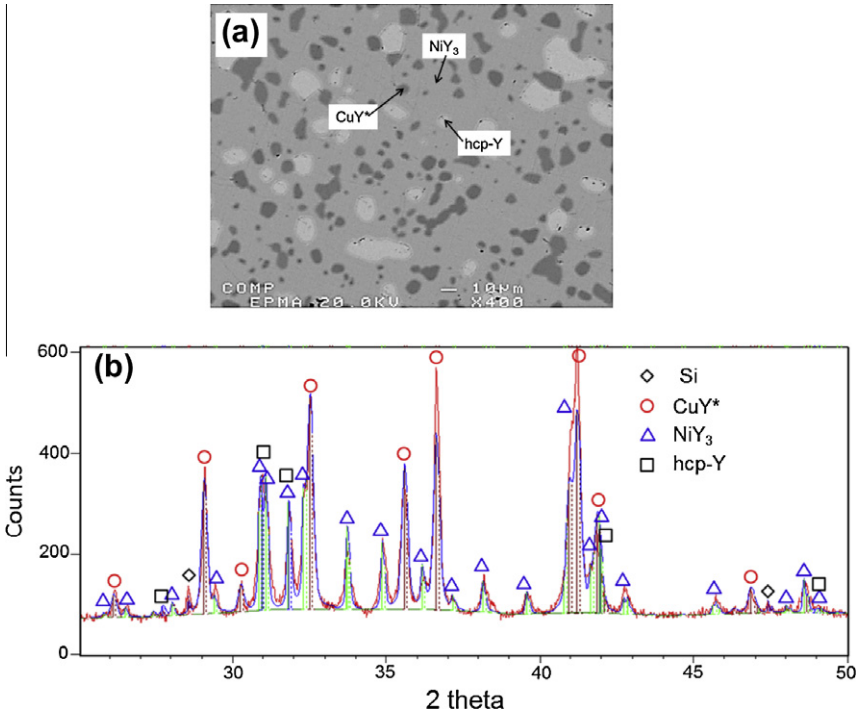

Fig. 6. (a) BSE image; and (b) XRD pattern of sample 1 (Cu/Ni/Y 16.08/8.69/75.23 at.%).

$Ni_3Y + Cu_2Y + Cu_4Y$ and $Ni_3Y + Cu_2Y + Ni_2Y$

These two three phase regions exit in the center of the phase diagram and are important to understand the phase relations in this system. Two key alloys (11 and 12) have been prepared to identify the phase relations and their WDS analysis has been summarized in Table 2. The BSE image of key alloy 12 is shown in Fig. 9. One of the common phases in these two regions is the Ni_3Y which is promising for the hydrogen storage application. Burnasheva and Tarasov [1], in their hydrogen storage work on the Cu–Ni–Y system, reported that they found one alloy $Cu_{0.5}Ni_{2.5}Y$ to be a single phase with the same crystal structure as that of Ni_3Y. Although this result does not provide the maximum solubility of Cu in Ni_3Y, it proves that this solubility should be at least 12.5 at.% Cu which is in accordance with the present work that finds the maximum solubility to be ~25 at.% Cu. There is a possibility for a two phase region ($Cu_2Y + Ni_3Y$) to exist between these two three phase regions. But it was not observed in the present work.

$Ni_5Y + Ni_{17}Y_2 + fcc$

Zheng and Nong [6] reported a three phase region among Ni_5Y, $Ni_{17}Y_2$ and fcc phase based on their XRD analysis. A three phase region has been observed here but with different composition of the Ni_5Y and fcc phase. The XRD pattern of the key alloy 26 (Cu/Ni/Y 43.94/45.99/10.07 at.%) is shown in Fig. 10. The WDS analysis of this alloy is shown in Table 2 which reveals that $Ni_{17}Y_2$ dissolves about 37 at.% Cu which is in good agreement with those of Zheng and Nong [6]. However, the Ni_5Y triangulation has been found at 31 at.% Cu whereas the fcc phase is found at 76 at.% Cu. The reported values by Zheng and Nong [6] were 39.16 and 67.76 at.% Cu, respectively.

3.2.2. Other three phase regions

There are four other three phase regions in the Cu–Ni–Y system which could not be identified clearly. They have been constructed based on the tendency of the phase development in the region. These are: $NiY + Ni_2Y_3 + NiY_3$, $Ni_3Y + Ni_7Y_2 + Ni_4Y$, $Cu_7Y_2 + Cu_2Y + Cu_4Y$ and $Cu_6Y + Cu_4Y + Ni_5Y$. All these three phase regions are expected to be present in the equilibrium phase diagram as the constituent compounds are stable in the binary systems at this temperature. These regions are very thin and it is very difficult to prepare alloys that lie in them. Therefore, they have been shown by dotted lines on the isothermal section in Fig. 5. Zheng and Nong [6] reported a three phase region among Ni_5Y, Cu_6Y and fcc phase based on their XRD analysis. This has been accepted in the current work.

3.3. Complete mutual solubility between CuY* and NiY

A complete solid solubility has been detected between CuY* and NiY although the room temperature crystal structure of CuY and NiY are CsCl and FeB types, respectively as can be seen in Table 1. Kadomatsu et al. [7] reported that CuY transforms from cubic CsCl

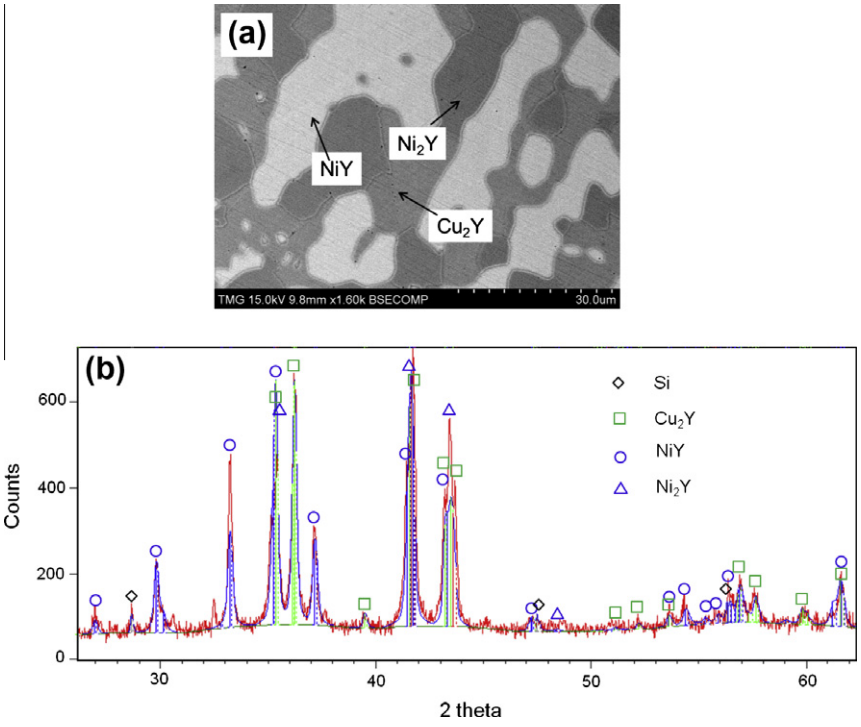

Fig. 7. (a) BSE image; and (b) XRD pattern of sample 6 (Cu/Ni/Y 18.15/41.98/39.88 at.%).

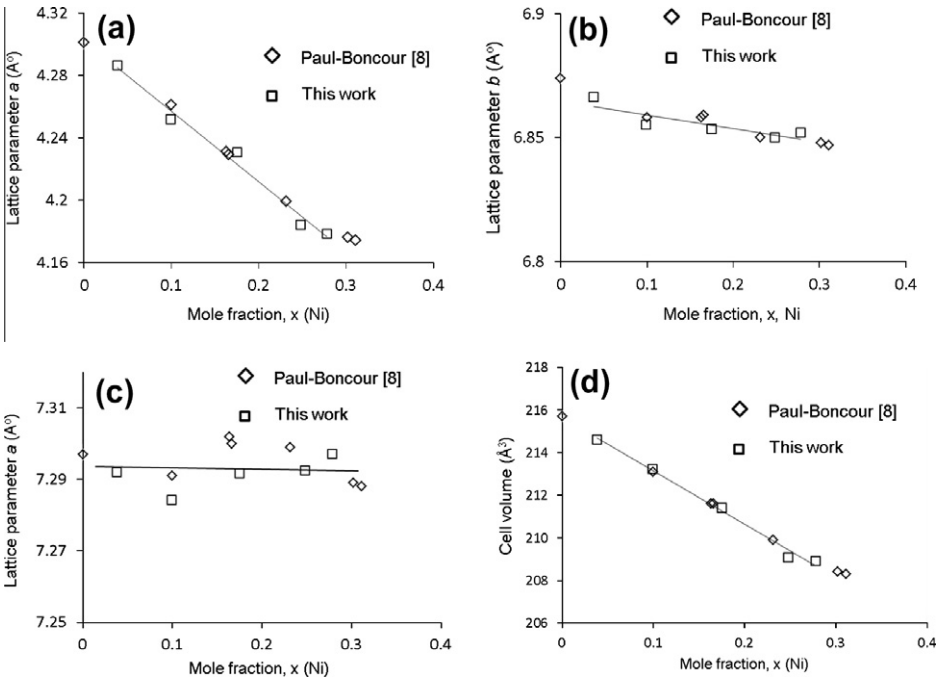

Fig. 8. Variation of lattice parameters of Cu_2Y as a function of x for the $Cu_{2-x}Ni_xY$ ($1.18 \leqslant x \leqslant 2$) alloys (a) lattice parameter *a*; (b) lattice parameter *b*; (c) lattice parameter *c*; and (d) variation of cell volume.

to tetragonal FeB type structure at lower temperature. This transformation temperature showed a large hysteresis during heating (510 °C) and cooling (−153 °C). Since NiY has FeB type structure, Gupta [10] suggested that a continuous solid solution between these two compounds could exist. Six key samples (1, 3, 4, 5, 6 and 7) have been prepared to investigate the solubility. The WDS measurements of these alloys are listed in Table 2. The phase relations are shown on the isothermal section in Fig. 5. The XRD patterns of these alloys match the FeB not the CsCl structure type. Also, if there is no continuous solubility, a three phase region should be present which could not be found. Therefore, a continuous solubility between CuY* and NiY is most likely to exist.

Refinement of the XRD pattern of the alloys containing NiY phase has been done using Rietveld analysis. The use of Si as an internal calibration standard enabled the correction for the zero shift and specimen displacement, which are the most serious sys-

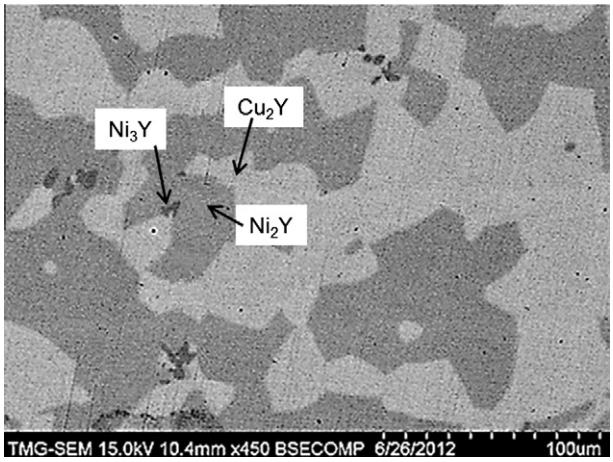

Fig. 9. BSE image of sample 12 (Cu/Ni/Y 25.10/44.23/30.67 at.%).

tematic errors in XRD results. Table 3 and Fig. 11 show the variation of cell parameters with Cu concentration for several samples (1, 4, 5, 6 and 7) where the substitution of Ni by Cu atom decreases the unit cell parameters *a* and *c* but it increases *b*. Table 3 lists the refined structural parameters of NiY and the reliability factors. The least-squares approximation is used to establish the relationships between the lattice parameters and Cu concentration. The atomic radii of Cu, Ni and Y are 128 pm, 124 pm and 180 pm, respectively. In the NiY ternary solubility region, Y content variation remains constant while substitution of Ni occurs by Cu atoms. According to the normal trend all the lattice parameters should increase with Cu concentration because Cu atoms are slightly larger than Ni which cannot be observed in this case. This can be explained by the increase of the lattice volume as can be seen in Fig. 11d. The small reduction in *a* and *c* parameters have been compensated by comparatively larger increase in the *b* parameter.

The coordination sphere and atomic substitution of Ni by Cu has been identified as can be seen in Fig. 12. The substitution sites have been labeled by M1 (sites of mixing). All the Ni atoms are on the 4c sites. M1 sites can be occupied either by Ni or Cu based on the Cu concentration. There will be no substitution on the Y sites. The bond length has been calculated for the samples 1 (Cu rich) and 7 (Ni rich) as listed in Table 4. It can be seen that the maximum change in bond length occurs for the M1–M1 atoms from 2.463 Å to 2.561 Å. This increase of length has been reflected in relatively large increment of the cell parameter *b*, from 4.164 to 4.418 Å. The bond length for all positions show increment except one of the M1–Y1 bond where it decreases from 2.850 to 2.818 Å. Because of this, cell parameters *a* and *c* decreased as can be seen in Fig. 11a and c.

3.4. Complete mutual solubility between Cu_4Y and Ni_4Y

Complete solubility between Cu_4Y and Ni_4Y has been observed from the XRD and WDS measurements of several key alloys. The WDS measurements of key alloys 9, 10, 11, 14, 15, 17, 18 and 24 in Table 2 show a stable phase with $Cu_xNi_{4-x}Y$ composition. Diffusion couple 2 (Fig. 4) also shows the presence of this phase from 30 to 40 at.% Cu. All these results indicate a complete solubility between Cu_4Y and Ni_4Y compounds. The primary condition for the formation of this kind of solubility between the constituents is having the same crystal structure. But unfortunately the crystal structure of Ni_4Y phase is not known. Therefore, it is decided to use the reference pattern of Cu_4Y to identify the Ni_4Y compound in the XRD results. The XRD patterns of three key alloys (15, 17 and 18) have been compared and shown in Fig. 13. Sample 15 (Cu/Ni/Y 77.99/3.48/15.53 at.%) is single phase consisting only of Cu_4Y. Sample 17 (Cu/Ni/Y 4.93/74.37/20.70 at.%) is composed of three phases, of Ni_4Y, Ni_3Y and Ni_7Y_2. Sample 18 (Cu/Ni/Y 6.48/73.92/19.60 at.%) has two phases; Ni_5Y and Ni_4Y. XRD patterns of both samples (17 and 18) show peaks belonging to Cu_4Y. However, Cu_4Y cannot be present in this sample because its composition is very close to the Ni–Y side. This indicates that most probably Ni_4Y has the same crystal structure as Cu_4Y. Further, it can be concluded that a complete solubility

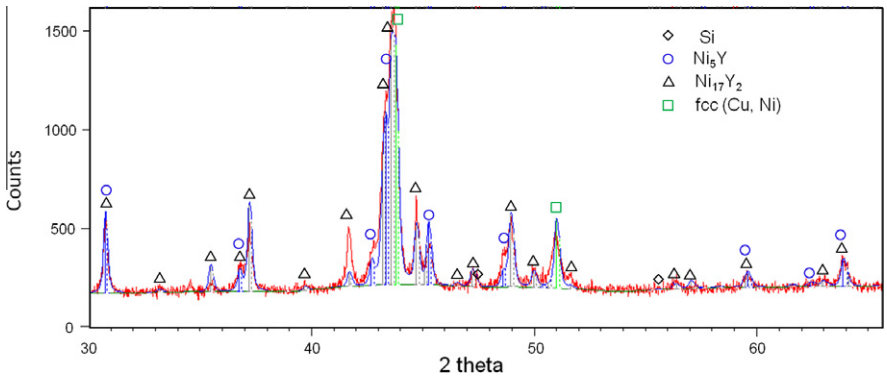

Fig. 10. XRD pattern of sample 26 (Cu/Ni/Y 43.94/45.99/10.07 at.%).

Table 3
The chemical compositions and unit cell parameters of NiY determined by WDS and Rietveld analysis.

Sample no.	Composition of NiY phase, EPMA data			Unit cell parameters and lattice volume				Reliability factors[a]		
	Cu	Ni	Y	*a* (Å)	*b* (Å)	*c* (Å)	V (Å^3)	R_e	R_{wp}	*s*
1	43.12	6.19	50.69	7.075	4.418	5.416	169.29	4.73	9.02	3.64
5	35.91	12.74	51.34	7.081	4.424	5.423	169.85	6.79	8.07	1.41
4	26.69	22.33	50.98	7.077	4.358	5.446	167.98	4.06	9.71	5.73
6	7.4	42.24	50.36	7.111	4.190	5.490	163.57	9.97	15.12	2.30
7	4.68	44.93	50.39	7.131	4.164	5.511	163.63	9.84	23.08	5.50

[a] Reliability factors: *s* is the goodness of fit, R_{wp} is the weighted summation of the residuals of the least-squares fit and R_e is the statistically expected value.

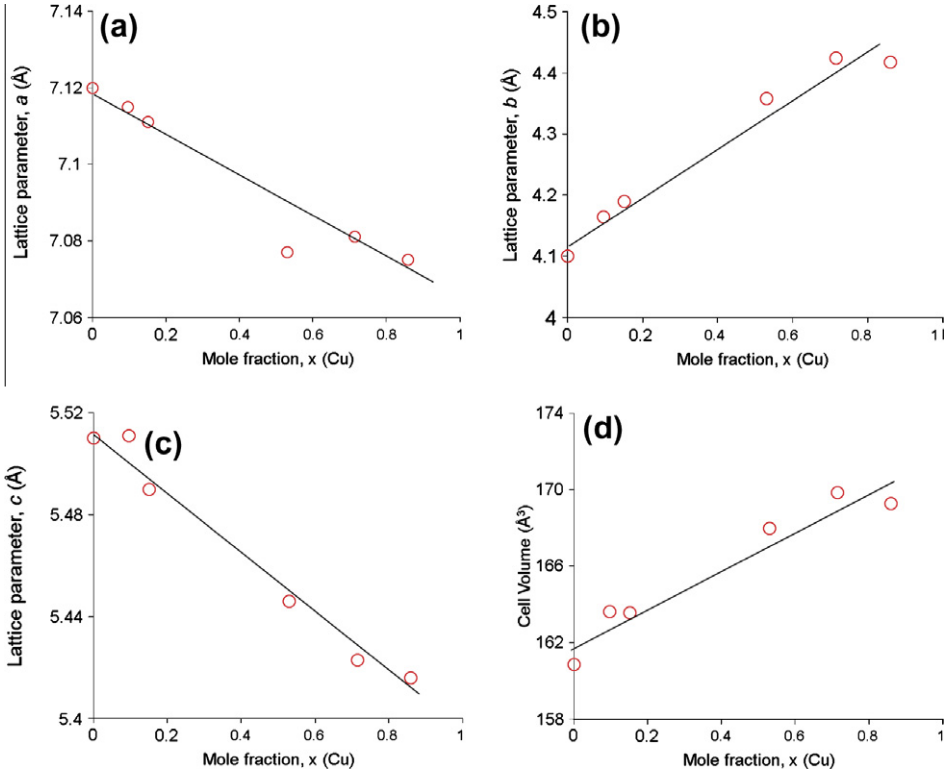

Fig. 11. Variation of lattice parameters of NiY as a function of x for the $Cu_xNi_{1-x}Y$ ($0 \leqslant x \leqslant 1$) alloys (a) lattice parameter a; (b) lattice parameter b; (c) lattice parameter c; and (d) cell volume.

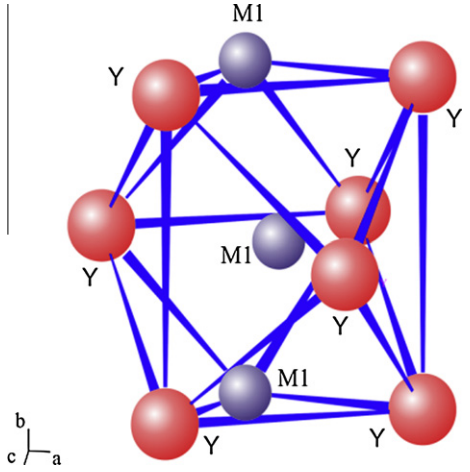

Fig. 12. The coordination spheres of a Ni atom of the NiY compound. The substitution sites of Ni by Cu have been denoted by M1.

Table 4
Atomic bond lengths of the NiY compound in samples 1 and 7.

Sample no.	Atom 1	Atom 2	Distance (Å)	Sample no.	Atom 1	Atom 2	Distance (Å)
7	M1	–M1	2.463	1	M1	–M1	2.561
	M1	–M1	2.463		M1	–M1	2.561
	M1	–Y1	2.850		M1	–Y1	2.818
	M1	–Y1	2.863		M1	–Y1	2.818
	M1	–Y1	2.906		M1	–Y1	2.970
	M1	–Y1	2.906		M1	–Y1	2.987
	M1	–Y1	2.973		M1	–Y1	2.987
	M1	–Y1	2.973		M1	–Y1	3.045
	M1	–Y1	3.018		M1	–Y1	3.045
	Y1	–M1	2.850		Y1	–M1	2.818
	Y1	–M1	2.863		Y1	–M1	2.818
	Y1	–M1	2.906		Y1	–M1	2.970
	Y1	–M1	2.906		Y1	–M1	2.987
	Y1	–M1	2.973		Y1	–M1	2.987
	Y1	–M1	2.973		Y1	–M1	3.045
	Y1	–M1	3.018		Y1	–M1	3.045

between Cu_4Y and Ni_4Y compounds exists. However, more crystallographic investigation needs to be done to verify this observation.

3.5. Partial solubility of Ni_5Y phase

The partial isothermal section at room temperature reported by Zheng and Nong [6] shows that Ni_5Y phase is stable until Cu_5Y composition. But Cu_5Y compound does not exist in the acceptable Cu–Y phase diagram [10]. Thus stability of the Ni_5Y phase up to the Cu_5Y composition is not possible. Dwight [9] examined the crystal structures of several alloys at the $Cu_xNi_{5-x}Y$ compositions. The $CaCu_5$ type structure was found to be stable from Ni_5Y to Cu_4NiY composition. Most probably Cu_5Y is a metastable phase which was stabilized by the addition of a small amount of Ni. Four key alloys, 20, 21, 22 and 23, have been prepared in this region to determine the solubility limit of Ni_5Y. All of these alloys contain Ni_5Y and fcc phases as can be seen in the BSE image of sample 20 (Cu/Ni/Y 81.78/8.46/9.74 at.%) in Fig. 14. Based on the WDS analysis of these alloys as listed in Table 2, it can be confirmed that Ni_5Y is stable at least until 72.4 at.% Cu. However, the maximum solubility of Ni_5Y could not be obtained in this work because of the presence of phases very close in composition such as of Cu_6Y and Cu_4Y. One alloy, sample 19 (Cu/Ni/Y 85.64/1.37/12.99 at.%) which has slightly more Cu concentration than sample 20 (Cu/Ni/Y 81.78/

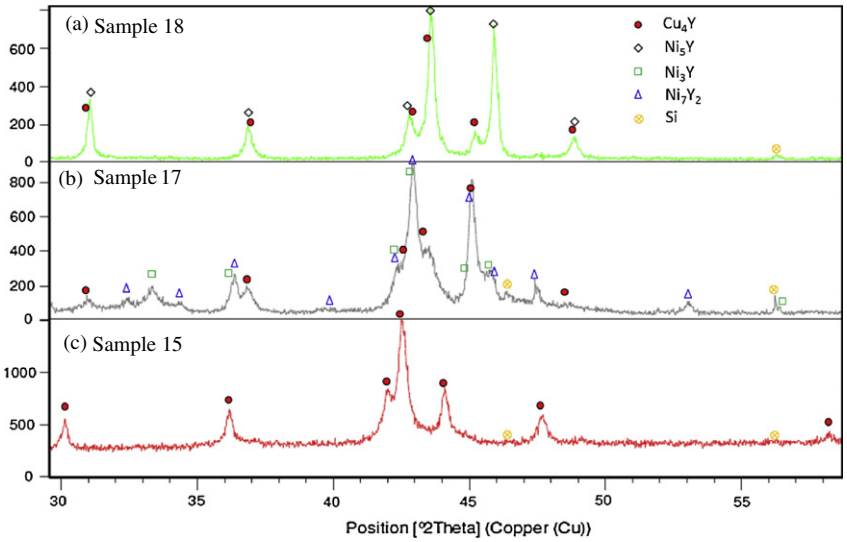

Fig. 13. XRD patterns of samples (a) 18 (Cu/Ni/Y 6.48/73.92/19.60 at.%); (b) 17 (Cu/Ni/Y 4.93/74.37/20.70 at.%); (c) 15 (Cu/Ni/Y 77.99/3.48/15.53 at.%) showing the effect of Cu_4Y–Ni_4Y extended solubility.

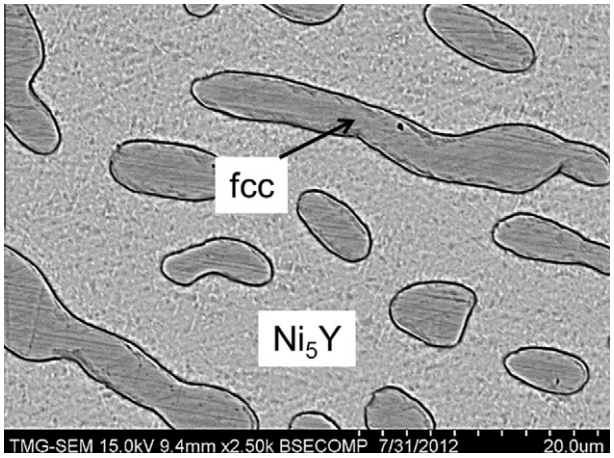

Fig. 14. BSE image of sample 20 (Cu/Ni/Y 81.78/8.46/9.74 at.%).

8.46/9.74 at.%) shows a single phase of Cu_6Y. Therefore, a three phase region containing Cu_6Y, Ni_5Y and Cu_4Y is assumed and drawn with a dotted line indicating that this region is not experimentally confirmed.

3.6. Ternary solubility of the fcc phase

Several key alloys (20, 23, 25, 26, 27 and 28) have been examined to estimate the solubility of Y in the fcc phase. None of these alloys show a solubility more than 0.6 at.% Y. The reported values by Zheng and Nong [6] was about 1.5 at.% Y which is higher than the present work. However, WDS analysis is more precise in determining the composition than the XRD analysis. Therefore, lower solubility of Y in the fcc phase is more likely.

Some other rare earth containing systems like Gd–Cu–Ni [16], Ho–Cu–Ni [17], La–Cu–Ni [18], and Ce–Cu–Ni [19] show that the compounds of (RE,Cu) or (RE,Ni) form complete or partial but significant solid solutions of Cu in (RE,Ni) or Ni in (RE,Cu) binary compounds. The ternary solid solubilities of these compounds are almost parallel to the Cu–Ni line keeping constant RE concentration. The same tendency has been observed in the Cu–Ni–Y system.

4. Summary

A comprehensive investigation of the Cu–Ni–Y system has been performed using XRD and WDS measurements of several key alloys. Two solid–solid diffusion couples have also been studied to identify the ternary solubilities of the binary intermetallic compounds and to understand the phase relations among them. Based on the key alloys and diffusion couple analysis, the isothermal section at 700 °C for the whole composition range of the Cu–Ni–Y system has been established. Rietveld analysis has been carried out for the XRD results and the variation of the lattice parameters has been reported for the NiY and Cu_2Y compounds. Continuous solubility between CuY*–NiY and Cu_4Y–Ni_4Y compounds has been identified. The maximum ternary solubility of NiY_3, Ni_2Y, Ni_3Y, $Ni_{17}Y_2$ and Cu_2Y has been determined. The solubility of Y in the fcc phase has been found to be ~0.6 at.%.

Acknowledgements

This research was carried out with the support of NSERC Alexander Graham Bell Canada Graduate Scholarship (NSERC CGS). The authors wish to express their appreciation for this support. The authors also like to acknowledge the help of Dmytro Kevorkov and Ahmad Omar Mostafa of Mechanical Engineering department, Concordia University, for useful discussions and suggestions.

References

[1] V.V. Burnasheva, B.P. Tarasov, Effect of the partial replacement of nickel or yttrium by other metals on hydrogen absorption by yttrium–nickel (YNi_3) compounds, Zhurnal Neorganicheskoi Khimii 29 (1984) 1136–1141.
[2] P.D. Carfagna, W.E. Wallace, R.S. Craig, Crystallographic and magnetic characteristics of the Y_2 $Ni_{17-x}Cu_x$ System, Journal of Solid State Chemistry 2 (1970) 1–5.
[3] Q.F. Li, K.Q. Qiu, X. Yang, Y.L. Ren, X.G. Yuan, T. Zhang, Glass forming ability and reliability in fracture stress for Mg–Cu–Ni–Nd–Y bulk metallic glasses, Materials Science and Engineering: A 491 (2008) 420–424.
[4] Y.L. Ren, J.H. Zuo, K.Q. Qiu, H.F. Zhang, Z.Q. Hu, Eutectic structure and bulk glass formation in Mg-based alloys, Intermetallics 12 (2004) 1205–1209.
[5] P. Villars, K. Cenzual, Pearson's Crystal Data – Crystal Structure Database for Inorganic Compounds (on CD-ROM), ASM International, Materials Park, OH, 2009.
[6] L. Zheng, J. Nong, A part of room temperature section of phase diagram of Y–Cu–Ni (Y ⩽ 16.7 at.%) system, Acta metallurgica Sinica 21 (1985) B58–B60.

[7] H. Kadomatsu, Y. Kawanishi, M. Kurisu, Structural phase transitions in $YCu_{1-x}\mu_x$ (M = Ni, Ag, and Ga), Jounal of Less Common Metals 141 (1988) 29–36.
[8] V. Paul-Boncour, A. Lindbaum, E. Gratz, E. Leroy, A. Percheron-Guégan, Structural study of the pseudobinary Y(Ni, $Cu)_2$ system, Intermetallics 10 (2002) 1011–1017.
[9] A.E. Dwight, Crystal structure of R.E.–Ni_4Au compounds and unit cell constants in the YCo_5–YNi_5–YCu_5 series, Jounal of Less Common Metals 43 (1975) 121–128.
[10] K. Gupta, The Cu–Ni–Y (Copper–Nickel–Yttrium) system, Journal of Phase Equilibria and Diffusion 30 (2009) 651–656.
[11] J.-C. Zhao, A combinatorial approach for structural materials, Advanced Engineering Materials 3 (2001) 143–147.
[12] J.-C. Zhao, A combinatorial approach for efficient mapping of phase diagrams and properties, Journal of Materials Research 16 (2001) 1565–1578.
[13] F.J.J. van Loo, Multiphase diffusion in binary and ternary solid-state systems, Progress in Solid State Chemistry 20 (1990) 47–99.
[14] A.A. Kodentsov, G.F. Bastin, F.J.J. Van Loo, The diffusion couple technique in phase diagram determination, Journal of Alloys and Compounds 320 (2001) 207–217.
[15] J.C. Zhao, M.R. Jackson, L.A. Peluso, Determination of the Nb–Cr–Si phase diagram using diffusion multiples, Acta Materialia 51 (2003) 6395–6405.
[16] Z. Huaiying, Z. Yinghong, G. Zhengfei, The isothermal section (500 °C) of the Gd–Cu–Ni ternary phase diagram, Journal of Alloys and Compounds 221 (1995) 98–101.
[17] Y. Zhuang, L. Zhang, The isothermal section (500 °C) of the phase diagram of the Cu–Ho–Ni ternary system, Journal of the Less Common Metals 170 (1991) 223–229.
[18] J. Liu, F. Ma, Y. Zhuang, F. Jiao, J. Yan, The isothermal section of the phase diagram of the La–Ni–Cu ternary system at 673 K, Journal of Alloys and Compounds 386 (2005) 174–176.
[19] J. Wang, A. Pisch, R. Flükiger, J.L. Jorda, Phase equilibrium in the cerium-poor Ce–Ni–Cu system, Journal of Alloys and Compounds 436 (2007) 161–169.